Stability Analysis of Large Wind Farms Connected to Weak AC Networks Incorporating PLL Dynamics

Kamyab Givaki, and Lie Xu

Department of Electronic and Electrical Engineering
University of Strathclyde
Glasgow, United Kingdom
k.givaki@strath.ac.uk; lie.xu@strath.ac.uk

Keywords: Phase locked loop, stability, vector current control, voltage source converter, wind farm.

Abstract

Voltage source converter interfaced wind turbines connected to weak grids can induce system instability. A state space model is used in this paper to study the stability of large wind farms. Dynamics of the phase locked loop is integrated to the state space model. The advantage of this model is that it allows study the stability of systems with parallel wind turbines. Studies on the dynamic responses of the system show the importance of including phase locked loop as its existence can induce system instability especially under weak network conditions. This model can be used to study the stability of converter interfaced wind farms and helps to design the converter controller to ensure wind farm system stability when connected to weak grids.

1 Introduction

Variable speed wind turbines that use voltage source converters (VSC) for connecting to power grids are widely used. Vector current control is the most commonly used method for controlling the interface VSCs, though problems can arise when the connected power network is weak and systems can potentially become unstable. Many wind farms are being constructed in remote areas where the wind speed is high but grid strength is low. In addition, it is possible that the impedance could increase further due to faults, variation in the load and line trips [1]. Different filter schemes for reducing harmonic contents can be used to connect VSCs to grids. Third order LCL filters are good options due to their low cost and size [2]. However, using LCL filters can make the control of current loop more difficult and make the closed loop system more likely to become unstable [3].

Many studies have been conducted to assess system stability of grid connected VSCs [2, 3]. However, in [2, 3] the dynamics of the phase locked loop (PLL), which can significantly affect system stability especially for weak networks[4], was not considered. In [5, 6] the analytical model of HVDC system is developed to study the stability of LCC-HVDC transmission link. In [5] the PLL is modelled by a state space representation and the PLL model in [5] is used in [7] to develop the analytical model of VSC-HVDC transmission. Also in [8] an analytical model of VSC-HVDC is developed which includes PLL dynamics expressed by a state-space model. However the d-axis voltage of the converter filter bus is selected as the reference for dq frame and thus, it becomes complicated when studying the dynamics of parallel converters since each converter has its own dq reference. Reference [9] tried to add PLL dynamics to converter dynamic model by using synchronous machines theory though the PLL dynamics was added to the feed forward grid voltage rather than to the converter voltage. In [10], the dynamics of PLL has been studied, but not as a part of the dynamic model of the VSC. The concept of Jacobean matrix of the AC grid is introduced in [11] which can be used to study VSC converters with power synchronization control but it doesn't include PLL dynamics.

To study the stability of multiple grid connected VSCs, a state space model is developed and the true dynamics of the PLL is integrated to the model. In the developed model, the d-axis of the synchronous frame is aligned to the source voltage (similar to voltage oriented control) and the filter bus voltage at VSC terminal is used to derive PLL dynamics. This ensures systems which contain a number of parallel connected VSCs can be modelled accurately by considering each PLL separately. The stability studies carried out by this model can be used to design converter control systems to ensure system stability especially when the converter system is connected to weak grids.
The paper is organized as follows. Dynamic system model including the PLL is described in Section II. In section 3, step response and root locus diagrams are used to assess the effect of PLL on system stability. Finally Section 4 draws the conclusions.

2 System modelling including multiple clusters of wind turbines

2.1 Converter model

Figure 1 shows a simplified circuit layout of a grid connected VSC where R_1 and L_1 are the resistance and inductance of the converter reactor, C is the filter capacitor, $L_{tx}$is the leakage inductance of the transformer. R_{net} and L_{net} represent the grid resistance and inductance, respectively. $\omega_b = 2\pi f_b$ is the base angular frequency of the system.

$$\frac{d}{dt}\begin{bmatrix} i_{1d} \\ i_{1q} \\ V_{Cd} \\ V_{Cq} \\ i_{2d} \\ i_{2q} \end{bmatrix} = \omega_b * \begin{bmatrix} -\frac{R_1}{L_1} & \omega & -\frac{1}{L_1} & 0 & 0 & 0 \\ -\omega & -\frac{R_1}{L_1} & 0 & -\frac{1}{L_1} & 0 & 0 \\ \frac{1}{C} & 0 & 0 & -\omega & -\frac{1}{C} & 0 \\ 0 & \frac{1}{C} & \omega & 0 & 0 & -\frac{1}{C} \\ 0 & 0 & \frac{1}{L_2} & 0 & -\frac{R_2}{L_2} & \omega \\ 0 & 0 & 0 & \frac{1}{L_2} & -\omega & -\frac{R_2}{L_2} \end{bmatrix} \begin{bmatrix} i_{1d} \\ i_{1q} \\ V_{Cd} \\ V_{Cq} \\ i_{2d} \\ i_{2q} \end{bmatrix} + \omega_b \begin{bmatrix} 0 & 0 & +\frac{1}{L_1} & 0 \\ 0 & 0 & 0 & +\frac{1}{L_1} \\ 0 & 0 & 0 & 0 \\ 0 & 0 & 0 & 0 \\ -\frac{1}{L_2} & 0 & 0 & 0 \\ 0 & -\frac{1}{L_2} & 0 & 0 \end{bmatrix} \begin{bmatrix} V_{sd} \\ V_{sq} \\ V_{convd} \\ V_{convq} \end{bmatrix}, Y = CX \quad (1)$$

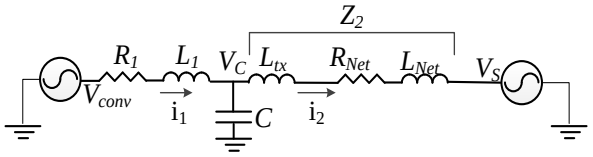

Figure 1. Schematic of VSC connected to power grid.

The equivalent circuit of the system shown in Figure 1 is presented in Figure 2 in the synchronous reference frame and equation (1) shows the state space representation of the system shown in Figure 2.

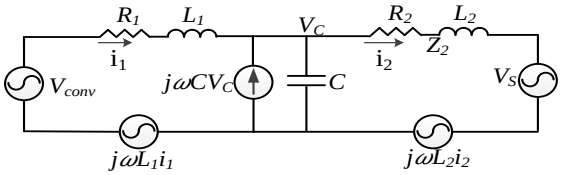

Figure 2. Equivalent circuit of grid connected VSC in dq frame.

Assuming a PI controller is used to control the converter current and its transfer function is given as

$$G_{PI} = K_p + \frac{K_i}{s} \quad (2)$$

where K_p and K_i are the proportional and integral gains of the PI controller, respectively. The converter modulation can usually be modelled as a unit delay equal to half of its switching period as:

$$G_{modulation} = \frac{1}{\tau.s+1} \quad (3)$$

where τ represents the modulation delay (i.e. τ =1/(2*f_{sw})).

The task of the PLL is to determine the voltage vector position at the converter filter bus, i.e., V_c. Under ideal situation the actual phase angle of V_c (θ_c in Figure 3) can be assumed to be the same as PLL measurement (θ_{PLL} in Figure 3). So in this case the phase error between the angle of the filter bus voltage and the PLL measurement is zero as shown in Figure 3(a). When a disturbance happens (e.g. a change in the current / power, etc.), the filter bus voltage V_C will change accordingly and misalignment will occur between the phase angle measured by the PLL and actual phase angle of Vc, leading to a phase angle error of Δθ between θ_C and θ_{PLL} (Figure 3(b)). As the real control system only sees θ_{PLL} thus to include the full dynamics of the PLL to the control system, the converter output voltage needs to be phase shifted by Δθ. A conventional PLL can be modeled by a PI controller and an integrator and its close loop transfer function of PLL is given as:

$$G_{PLL}(s) = \frac{k_{p-PLL}.s+k_{i-PLL}}{s^2+k_{p-PLL}.s+k_{i-PLL}} \quad (4)$$

where k_{p-PLL} and k_{i-PLL} are the proportional and integral gains of the PI controller, respectively.

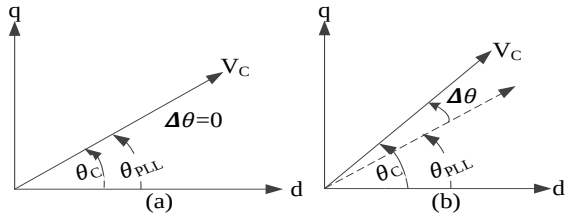

Figure 3. Positions of the actual and PLL measured filter bus voltage

In [12] a model of AC side voltage on the dynamic model of LCC converters is presented. In this model the phase angle of AC side voltage is used to calculate the phase difference between the actual voltage phase angle and PLL output, and this phase difference is then added to the firing angles. The same concept will be used in this paper to calculate the phase difference but the phase difference will be used to rotate the converter output voltage.

In the state space model shown in (1), V_C is one of the outputs and it is also used as the feed-forward term. As previously described, the phase error between the PLL measurement and the filter bus voltage are used to rotate the converter output terminal voltage vector as schematically shown in Figure 4. As shown, the phase angle rotation is shown as $e^{j\Delta\theta}$ and a new vector for converter terminal voltage is then obtained (V'_{conv}).

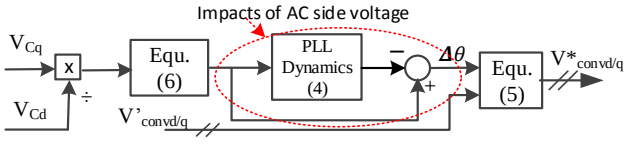

Figure 4. Simplified schematic of rotation because of PLL.

Considering the angle error is usually fairly small, the rotating of the converter voltage can be simplified as (5).

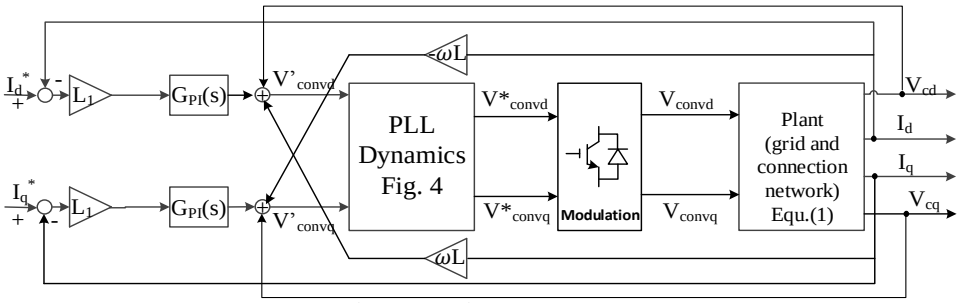

Figure 5. Block diagram of dynamics of the system integrated with PLL dynamics

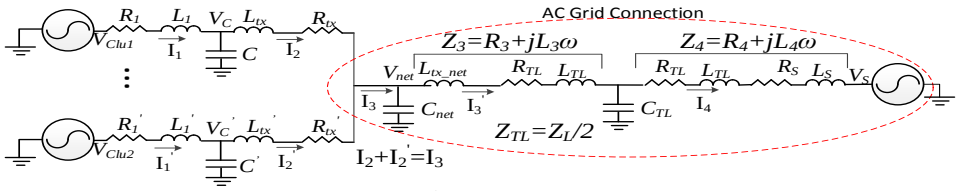

Figure 6. Single line diagram of two parallel converters with T line model

$$e^{j\Delta\theta} = \begin{bmatrix} \cos\Delta\theta & -\sin\Delta\theta \\ \sin\Delta\theta & \cos\Delta\theta \end{bmatrix} \approx \begin{bmatrix} 1 & -\Delta\theta \\ \Delta\theta & 1 \end{bmatrix} \quad (5)$$

Similarly, due to the small angle error, the inverse tan function (atan$\Delta\theta$) can be linearized as:

$$\Delta\theta = \text{atan}\left(\frac{V_{cq}}{V_{cd}}\right) \approx \left(\frac{V_{cq}}{V_{cd}}\right) \quad (6)$$

The final block diagram of the grid connected VSC with integrated PLL dynamics is shown in Figure 5.

2.2 Cluster model

In this section the dynamic model of parallel clusters of VSC is developed. Figure 6 shows the single line circuit of two parallel converters connected to the power grid through a step-up transformer (modelled as the inductance of L_{tx_net}) and transmission lines. The model developed in Section 2.1 is used to model each cluster of the VSCs. As the output of each cluster is current which is then connected to an inductor (transformer inductance), it is not allowed in simulation to connect current source to inductor (also modelled as current source). Thus, a very small capacitor (C_{net}) is added to the model as shown in Figure 6. Transmission line is modelled as a simple T section as shown in Figure 6. Pi equivalent of transmission line could also be used but with T section model, the order of the state space system will reduce by 4 (80 less elements) which reduces the complexity of the state space model as well as the computation requirements. The state space model of the AC grid connection consists of 8 states. Equation (7) shows the state space model of the AC grid connection. The schematic diagram of the cluster model of the system is shown in Figure 7.

The states parameters of the AC grid connection are the voltages of the capacitors C_{net} and C_{TL}, and the currents flow through the inductances L_3 and L_4 (Figure 6). V_{s_d} and V_{s_q} in Figure 7 are the d and q-axis voltages of the grid and as the grid voltage is aligned to the d axis, $V_{s_d} = 1\,p.u.$ and $V_{s_q} = 0$. By choosing the d-axis grid voltage as the reference instead of the output voltage of each cluster, multiple clusters of converters can be easily added in the model. So each cluster will be a stand-alone state space model which is connected to the AC grid connection state space model.

As shown in Figure 7 the output currents of the clusters are the inputs for the AC grid connection state space model. It is possible to study the stability of any numbers of parallel clusters of turbines that are connected to grid as long as the output current of all the clusters are available.

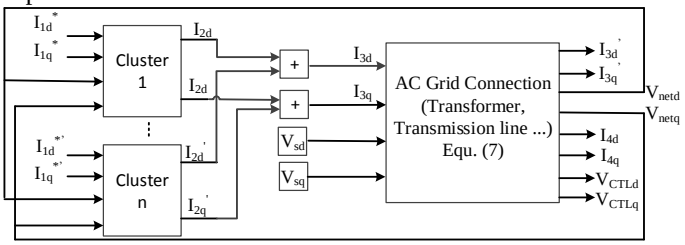

Figure 7. Block diagram of dynamic model of parallel converters

3 Model assessment and results

The state-space model that was developed in Section 2 is now used to study the stability of the converter connected to the grid and the impact of various parameters on system stability. The results for single converter are presented first and then the parallel converter results will be discussed. The parameters of the studied system are given in Appendix. It should be noted that in each part all the parameters are constant other than the one that is being studied. The converter model represents 10 fully rated wind turbines which are connected to the power grid through voltage source converters.

Figures 8 and 9 show the step responses of the d-axis current for the state space model and the time domain model (developed using Simulink) for different SCR values (3-10) and controller bandwidth (20-100Hz), respectively.

$$\frac{d}{dt}\begin{bmatrix} i'_{3d} \\ i'_{3q} \\ V_{net_d} \\ V_{net_q} \\ i_{4_d} \\ i_{4_q} \\ V_{CT_d} \\ V_{CT_q} \end{bmatrix} = \omega_b * \begin{bmatrix} -\frac{r_3}{L_3} & w & \frac{1}{L_3} & 0 & 0 & 0 & -\frac{1}{L_3} & 0 \\ -w & -\frac{r_3}{L_3} & 0 & \frac{1}{L_3} & 0 & 0 & 0 & -\frac{1}{L_3} \\ -\frac{1}{c_{net}} & 0 & 0 & -w & 0 & 0 & 0 & 0 \\ 0 & -\frac{1}{c_{net}} & w & 0 & 0 & 0 & 0 & 0 \\ 0 & 0 & 0 & 0 & -\frac{r_4}{L_4} & w & \frac{1}{L_4} & 0 \\ 0 & 0 & 0 & 0 & -w & -\frac{r_4}{L_4} & 0 & \frac{1}{L_4} \\ \frac{1}{c_{TL}} & 0 & 0 & 0 & -\frac{1}{c_{TL}} & 0 & 0 & -w \\ 0 & \frac{1}{c_{TL}} & 0 & 0 & 0 & -\frac{1}{c_{TL}} & w & 0 \end{bmatrix} \begin{bmatrix} i'_{3d} \\ i'_{3q} \\ V_{net_d} \\ V_{net_q} \\ i_{4_d} \\ i_{4_q} \\ V_{CTL_d} \\ V_{CTL_q} \end{bmatrix} + \omega_b * \begin{bmatrix} 0 & 0 & 0 & 0 \\ 0 & 0 & 0 & 0 \\ \frac{1}{c_{net}} & 0 & 0 & 0 \\ 0 & \frac{1}{c_{net}} & 0 & 0 \\ 0 & 0 & -\frac{1}{L_4} & 0 \\ 0 & 0 & 0 & -\frac{1}{L_4} \\ 0 & 0 & 0 & 0 \\ 0 & 0 & 0 & 0 \end{bmatrix} \begin{bmatrix} i_{3_d} \\ i_{3_q} \\ V_{s_d} \\ V_{s_q} \end{bmatrix}, Y = CX \quad (7)$$

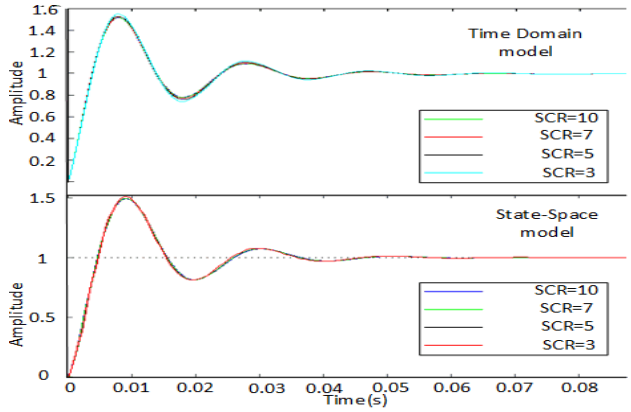

Figure 8. d-axis current step response for different SCR when $F_n = 50Hz$.

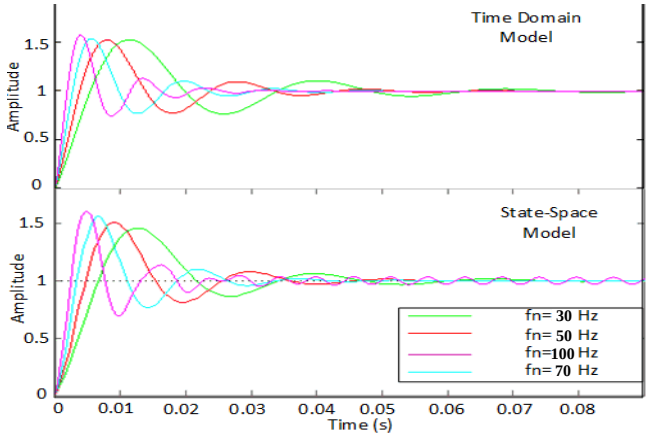

Figure 9. d-axis current step response for different controller bandwidth when SCR=5.

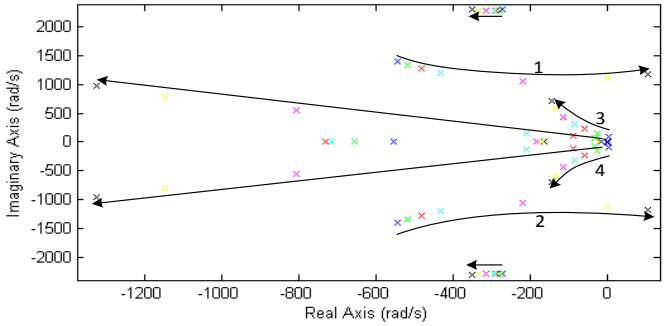

Figure 10. d-axis current transfer function poles for different controller bandwidth when SCR=5.

As can be seen from Figures 8 and 9, the dynamic performances for the time domain model and the state-space model are very similar which indicates that the state-space model represents the dynamics of the system very well.
It should be mentioned that in Figure 8, grid connection is relatively strong and the impedance of the grid is fairly small compared to the converter coupling reactor and step up transformer impedance. Thus the variations of the source SCR have negligible impacts on the step response.

Figure 10 shows the poles distribution (root locus) of the d-axis current transfer function of the single converter for different controller bandwidth. As can be seen in figure 11, the major poles that influence the dynamic behaviour of the system are grouped in different groups. Group 1 and group 3 of the poles are complex conjugate of the poles in group 2 and 4, respectively. The directions of arrows show the movement of poles locus with increasing of the controller bandwidth. Pole in group 1 and 2 tend to move to the instability region if the controller bandwidth increases (becomes unstable if $F_n > 110Hz$). In contrast group 3 and 4 poles tend to become unstable if the bandwidth decreases (becomes unstable if $F_n < 15Hz$.)

Figure 11 shows the root locus of the d-axis current of a single converter for SCR variation. The directions of the arrows show the movement of the poles locus when decreasing the SCR. Poles in group 1 and 2 are the dominant poles in order to measure the stability of the system. As can be seen in Figure 11 if the SCR decreases (SCR < 2.5) the system becomes unstable. It should be noted that this 'critical' value of SCR is based on the controller parameters and can be decreased by further tuning of the current controller.

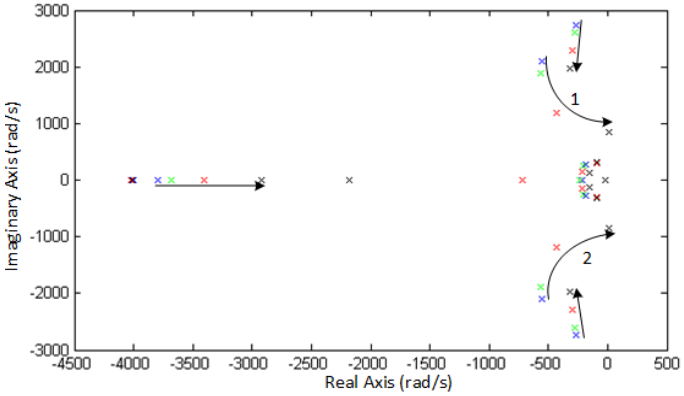

Figure 11. d-axis current transfer function poles for different SCR when $F_n = 50Hz$.

Figure 12 shows the d-axis current step responses for the time domain and state-space models when two clusters of wind turbines are considered in a wind farm. As can be seen in Figure 12, the step responses are very similar and it means that the state-space model is good enough to represent the wind farm in the stability studies. In Figure 12, the difference between two responses is due to the saturations in the time domain model that was not considered in the state-space model because of its non-linear characteristic. Figure 13 shows the poles distribution for the d-axis current transfer function of cluster 1 when the SCR varies. The full system is from 32nd order.

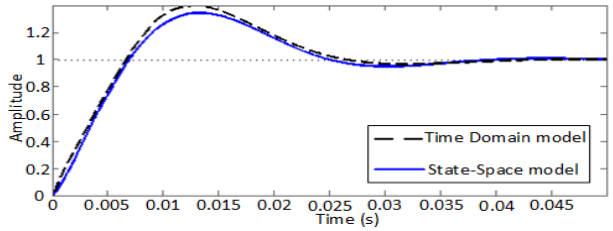

Figure 12. d-axis current step response for cluster 1 in the multiple cluster wind farm for SCR=5 and $F_n = 30Hz$.

The poles that affect the stability of the system are marked in 2 groups which are complex conjugate. The directions of the arrows show the locus with decreasing the SCR. As can be seen in Figure 13, the poles tend to move to unstable region if the grid connection becomes weaker (becomes unstable when SCR < 3.1). Therefore, it can be concluded that it is more likely for parallel converters to become unstable compared to a single converter if the connection to grid is weak.

Figure 14 further shows the major poles distribution of d-axis current transfer function for cluster 1 when the current controller bandwidth varies. As can be seen in Figure 14, there are 4 groups of major poles. The trend in the poles is the same as the trend in Figure 10. It is interesting to mention that with multiple converters (wind turbines) the current controller bandwidth has to be further limited. The controller becomes unstable if $F_n > 70Hz$ (due to group 3 and 4 poles) and $F_n < 20Hz$ (due to group 1 and 2 poles).

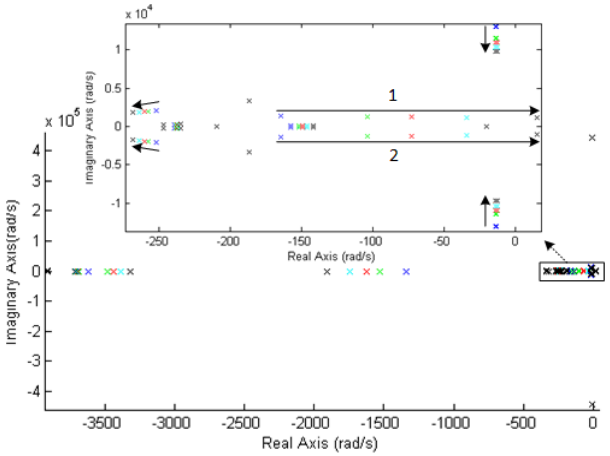

Figure 13. Poles distribution of d-axis current transfer function for cluster 1 in parallel converter structure, $F_n = 30Hz$ for different SCRs.

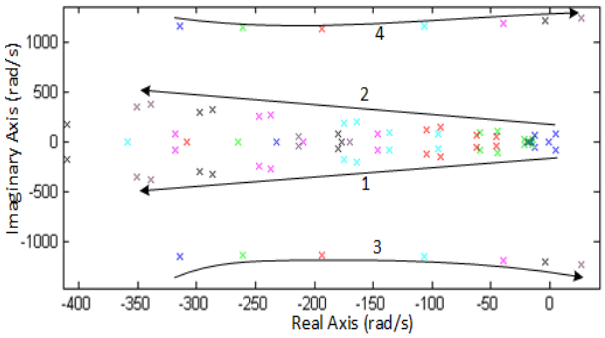

Figure 14. Major poles distribution of d-axis current transfer function for cluster 1 in parallel converter structure, SCR=5 for different controller bandwidth.

4 Conclusions

In this paper, a method to integrate the dynamics of phase locked loop to the state space model of a grid connected voltage source converter is introduced for assessing system stability. The propose method provides a convenient way for studying the stability of parallel VSCs connected to the same grid point via various connection lines. The main advantage of proposed dynamic model is to allow the study of the system stability during planning stage.

The impacts of the grid strength and current controller bandwidth on system stability have been analysed. The results show that with multiple converters, current controller bandwidth has to be limited.

Acknowledgements

This work is supported in part by EPSRC, project reference number EP/G037728/1.

Appendix

Parameter	Value
l_1 and l_1'	0.2 p.u.
l_{tx} and l_{tx}'	0.1 p.u.
C and C'	0.1 p.u.
f_b	50 Hz
$l_{tx\ net}$	0.1 p.u.
Number of turbines in a cluster	10
Wind turbine rating	3MW

Table 1. Model parameters

References

[1] N. P. W. Strachan, D. Jovcic, "Stability of a variable-speed permanent magnet wind generator with weak AC grids", *IEEE Trans. Power Delivery*, vol. 25, no. 4, pp. 2779-2788, (2010).

[2] H. Azani, A. Massoud, L. Benbrahim, B.W. Williams, D. Holiday, "An LCL filter-based grid-interfaced three-phase voltage source inverter: Performance evaluation

and stability analysis", in *Proc. 2014 7th IET International Conf. on Power Electronics, Machines and Drives*, Manchester.

[3] F. Tang, X. Jin, X. Zhou, Y. Tong, "Stability analysis on parallel of LCL-filter-based grid-connected converters in MW-level direct-drive wind generation using complex vector", in *Proc. 2011 International Conf. on Electrical Machines and Systems*, Beijing.

[4] L. Zhang, L. Harnefors, H. P. Nee, "Power-synchronization control of grid connected voltage source converters", IEEE Trans. Power System, vol. 25, no. 2, pp. 809–819, (2010).

[5] D. Jovcic, N. Pahalawaththa, M. Zavahir, "Analytical modelling of HVDC-HVAC systems", *IEEE Trans. Power Delivery*, vol.14, no. 2, pp 506-511, (1999).

[6] C. Osauskas, A. Wood, "Small-signal dynamic modelling of HVDC systems", *IEEE Trans. Power Delivery*, vol. 18, no. 1, pp.220-225, (2003).

[7] D. Jovcic, L.A. Lamont, L. Xu, "VSC transmission model for analytical studies", in *Proc. 2003 IEEE Power Engineering Society General Meeting*.

[8] M. Durrant, H. Werner, K. Abbott, "Model of a VSC HVDC terminal attached to a weak AC system", in *Proc. 2003 IEEE Conference on Control Applications*.

[9] C. Debruyne, S. Derammelaere, J. Desmet, L. Vandevelde, "Using general synchronous machine theory to integrate PLL controller dynamics into a static power electronic converter model", in Proc. *2012 IEEE Industry Applications Society Annual Meeting (IAS)*, Las Vegas.

[10] V. Kaura, V. Blasko, "Operation of a phase locked loop system under distorted utility conditions", *IEEE Trans. Industry Applications*, vol. 33, no.1, pp. 58-63, (1997).

[11] L. Zhang, L. Harnefors, H.P. Nee, "Interconnection of two very weak AC systems by VSC-HVDC links using power synchronization control", *IEEE Trans. Power System*, vol. 26, no. 1, pp.344-355, (2011).

[12] D. Jovcic, "Control of High Voltage DC and Flexible AC Transmission Systems," Ph.D. dissertation, Univ. Auckland, (1999).